AIP Journal of Applied Physics

Tunability of terahertz random lasers with temperature based on superconducting materials

Abbas Ghasempour Ardakani, Ali Reza Bahrampour, Seyed Mohammad Mahdavi, and Mehdi Hosseini

Citation: Journal of Applied Physics **112**, 043111 (2012); doi: 10.1063/1.4747837
View online: http://dx.doi.org/10.1063/1.4747837
View Table of Contents: http://scitation.aip.org/content/aip/journal/jap/112/4?ver=pdfcov
Published by the AIP Publishing

Tunability of terahertz random lasers with temperature based on superconducting materials

Abbas Ghasempour Ardakani,[1] Ali Reza Bahrampour,[1,a)] Seyed Mohammad Mahdavi,[1,2,a)] and Mehdi Hosseini[1,b)]
[1]*Department of Physics, Sharif University of Technology, Tehran, Iran*
[2]*Institute for Nanoscience and Nanotechnology, Sharif University of Technology, Tehran, Iran*

(Received 20 March 2012; accepted 9 August 2012; published online 31 August 2012)

We theoretically demonstrate the tunabiltiy of terahertz random lasers composed of high temperature superconductor YBCO and ruby layers as active medium. The considered system is a one-dimensional disordered medium made of ruby grain and YBCO. Finite-difference time domain method is used to calculate the emission spectrum and spatial distribution of electric field at different temperatures. Our numerical results reveal that the superconductor based random lasers exhibit large temperature tunability in the terahertz domain. The emission spectrum is significantly temperature dependent, the number of lasing modes and their intensities increase with decreasing temperature. Also, we make some discussion to explain the reason for the observed tunability and the effect of temperature variation on the spatial distribution of the electric field in the disordered active medium. © *2012 American Institute of Physics*. [http://dx.doi.org/10.1063/1.4747837]

I. INTRODUCTION

After the pioneering idea of random lasers (RLs) was firstly brought forward by Letokhov in 1968,[1] the first experimental observation of them was reported in 1986.[2] Since then, RLs have attracted great interest in two past decades.[3–18] In contrast to conventional lasers, there are no Fabry-Prot cavities in RLs and their feedback is provided by multiple scattering in disordered media. Simple and low cost fabrication of RLs makes them a promising coherent source in photonic applications. In recent years, several approaches have been suggested for description of RLs.[7–12] Among them, a time dependent model was presented by Jiang and Soukoulis in which Maxwell-Bloch equations are solved numerically by using finite-difference time domain (FDTD) method for one-dimensional (1D) case,[13] and it was extended by Sebbah and Vanneste to two-dimensional (2D) case.[14] Many properties of random lasers can be explained by this model.[15–18] It should be noted that the terahertz (THz) radiation has many applications, such as real time imaging,[19] heterodyne detection,[20] sensing and spectroscopy.[21] The importance of using THz spectral region in these applications is due to the fact that wavelength of rotational and vibrational transitions lies in this region. By exploiting this fact in characteristics absorption, distinction between different molecules is possible. Note that in these applications, it is necessary to use narrow band source with high emission powers. In recent years, many terahertz lasers have been fabricated, such as THz quantum cascade lasers (THz-QCL),[22] active photonic crystal lasers,[23] and methanol THz-laser.[24] Recently, Liu *et al*. proposed a terahertz random laser using ruby grains as active medium.[25] Construction of a terahertz random laser not only reduces the fabrication cost of the coherent terahertz source but also provides an observation path to observe photon localization in the terahertz region. With respect to different applications, it is advantageous to obtain tunable THz-RLs. In the previous scheme demonstrated in Ref. 25, once the RL was constructed, there was no external control on its emission spectrum. So far, several methods have been reported for tuning of RLs. Tuning of the output of random laser with temperature was demonstrated by Lawandy using a dye dissolved in polymethylmetalcrylate matrix.[26] Another scheme was also reported by Wiersma and Cavalieri, they made a liquid crystal based random laser, in which minor change in the temperature led to significant change in the laser emission behavior.[27] Gottardo *et al*. showed that optical resonance can provide an element to control random lasers.[28] Also, Lee *et al*. demonstrated electrically controllable RLs in a dye-doped liquid crystal cells with and without azo-dye.[29]

To obtain tunable THz-RLs, the electric permittivity or magnetic permeability of their constituents must depend on some external parameters. The dielectric constant of superconducting materials is strongly temperature dependent, which implies that temperature tunable THz-RLs made of superconducting materials are predictable. That is, the emission spectrum can be controlled by the ambient temperature. We have proposed a tunable random laser in optical region using superconductor (SC) layers in our previous work.[30] Moreover, tunable photonic crystals have been realized utilizing superconducting elements.[31–36] In this paper, we theoretically investigate THz-RLs composed of superconducting elements as their passive constituents. The electromagnetic fields in time domain are calculated using FDTD method at different temperatures. Through Fourier transformation of the recorded fields, spectral intensities are obtained. Our calculated results reveal that the emission spectrum of the THz-RLs can be altered with the ambient temperature.

Remaining parts of this paper are organized as follows. In Sec. II, we introduce a general form of time dependent theory in one-dimensional case in the presence of dispersive

[a)]Authors to whom correspondence should be addressed. Electronic addresses: bahrampour.alireza@yahoo.com and mahdavi@sharif.edu.
[b)]Present address: Department of Physics, Shiraz University of Technology, Shiraz, Iran.

superconducting elements. In Sec. III, we calculate the spectral intensity and the spatial distribution of electric fields for different temperature values. Finally, the paper is concluded in Sec. IV with some conclusions.

II. THEORETICAL METHOD

Herein, we consider a random one-dimensional system which is composed of binary layers consisted of two materials with different dielectric constant. A schematic of the random system is shown in Fig. 1 where the white layers with dielectric constant of $\varepsilon_{SC}(\omega)$ and the same thickness of d_{sn} simulate the superconducting materials (YBCO). The blue layers in Fig. 1 with dielectric constant of $\varepsilon = 10$ and random variable thickness of d_{gn} simulate active or gain media (ruby grain). The values of d_{gn} are randomly selected in the range of 20 to 80 μm and d_{sn} is taken to be 120 μm. We first select the length of the random system to be 3×10^4 μm. Then, YBCO layers with fixed thickness and ruby grain layers with random variable thickness are located in the length of the system such that they cover the whole of system length. The system considered here consists of 175 pairs of such binary layers.

For one-dimensional isotropic, non-magnetic active media, the Maxwell's equations are

$$\frac{\partial E(x,t)}{\partial x} = \mu_0 \frac{\partial H(x,t)}{\partial t}, \tag{1}$$

$$\frac{\partial H(x,t)}{\partial x} = \frac{\partial D(x,t)}{\partial t} + \frac{\partial P_{transition}(x,t)}{\partial t}, \tag{2}$$

where $P_{transition}$ is the polarization density due to the specific atomic transition from which gain or amplification is obtained; By setting $P_{transition} = 0$, the above equations can be used for passive medium; D is the electric displacement.

In the SC materials for simplicity, we consider the electro-magnetic property by using the two-liquid Gorter-Kazimir model, which describes the system as an admixture of two independent carrier liquids, the superconducting and the normal electrons:[35–38]

$$\varepsilon(\omega) = \left\{ 1 - \frac{\omega_{ps}^2}{\omega^2} - \frac{\omega_{pn}^2}{\omega[\omega + i\gamma]} \right\}, \tag{3}$$

where $\omega_{ps} = c/[\lambda\sqrt{\varepsilon_0}]$ and $\omega_{pn} = \sqrt{n_n e^2/[m\varepsilon_0]}$ are the plasma frequency of superconductor and normal materials, respectively; $\lambda = \sqrt{m/e^2 n_s \mu_0}$ is the London penetration depth. Here, n_n and n_s are normal and super electron concentration, respectively.

The mechanism of superconductor behavior which involves both the normal quasi-particles and the superconductor cooper pairs is described by the well-known two-fluid model.[39] As it is clear for low (LTS) and high temperature superconductors (HTS) materials, the normal

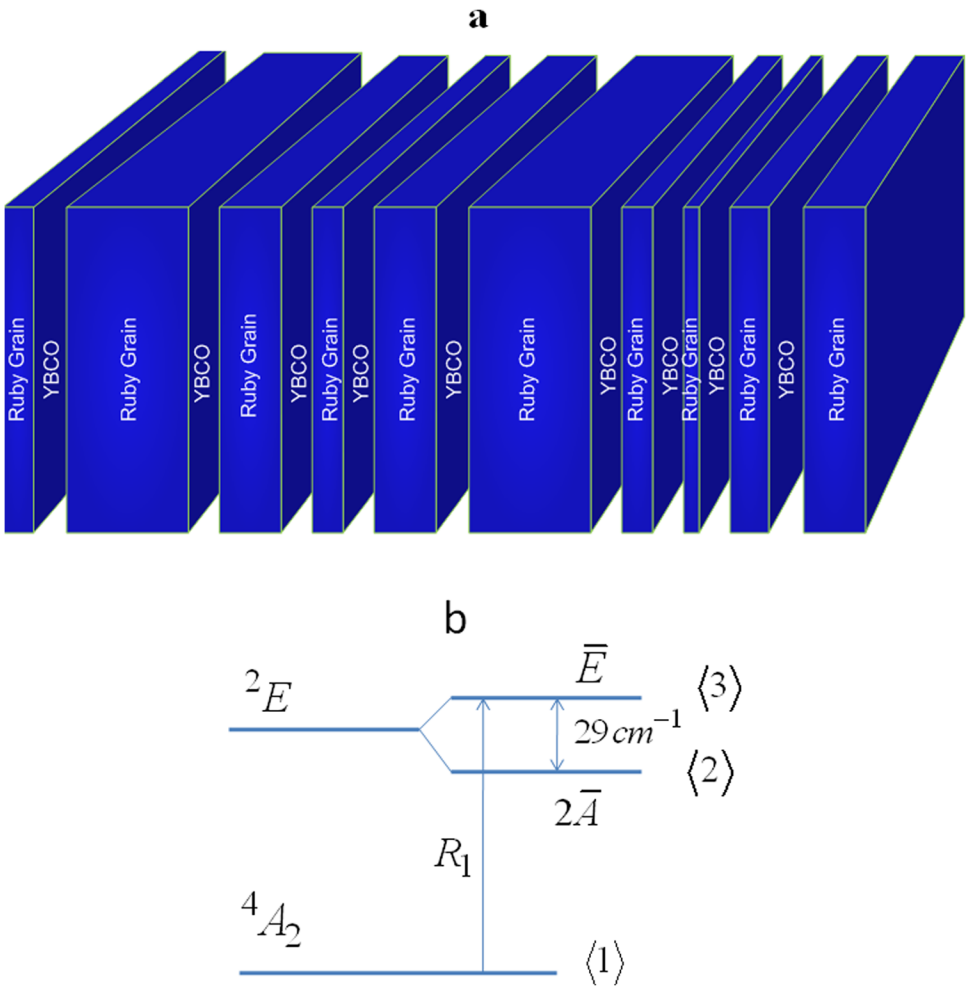

FIG. 1. Schematic of one dimensional random system in which the white and blue layers simulate the SC and active layers, respectively (a), schematic of the energy levels of ruby (b).

and superconductor carrier density depend on temperature,[40–42] so the plasma frequency is also temperature dependent:[40–42]

$$n_s(T) = n_t(1 - t^\beta), \tag{4}$$

where $n_n(T) = n_t t^\beta$ and $t = T/T_c$; $\beta \approx 4$ for LTS, $\beta \approx 2$ for HTS, and n_t is the total number of carriers in the superconductor material. By applying these experimental results in plasma frequencies for superconductor regions, it is easily found that $\omega_{ps} = \sqrt{e^2 n_t(1 - t^\beta)/m\varepsilon_0}$, $\omega_{pn} = \sqrt{n_t t^\beta e^2/m\varepsilon_0}$, so the dielectric constant of the superconductor layer is obtained as follows:

$$\varepsilon_{SC}(\omega) = 1 - \omega_p^2 \left\{ \frac{\alpha}{\omega^2} + \frac{1-\alpha}{\omega[\omega + i\gamma]} \right\}, \tag{5}$$

where $\alpha = 1 - t^\beta$ is the superconducting fluid fraction; $\omega_p = \sqrt{e^2 n_t/m\varepsilon_0}$ is the plasma frequency corresponding to the total electron density. The validity of Eq. (5) is for the frequencies lower than the superconductor gap frequency. At the frequencies higher than the given frequency, the superconductors behave like conventional metals. For YBCO which is considered here, the frequency should be lower than 3.43 THz.[38] So, the center frequency of gain line-shape must be chosen lower than the mentioned frequency. The dielectric constants of two layers in one-dimensional random system are given as

$$\varepsilon(x,\omega) = \begin{cases} 10 & \text{for active medium} \\ \varepsilon_{SC}(\omega) & \text{for supercinducting medium.} \end{cases} \tag{6}$$

Therefore, the dielectric constant of the superconducting materials can be tuned by changing the temperature. In order to simulate the superconductor layers as dispersive media in FDTD, Eq. (6) must be put into the sampled time domain.

Ruby grain is selected as an active medium which is described by the three-level rate equations as shown in Fig. 1(b). In ruby, the R_1 and R_2 lines arise from transition between the ground state of Cr^{3+} ion ($^4A^2$) to the first excited state (^2E). Spitting of these cubic-field states occurs due to trigonal crystal field and spin-orbit coupling. After splitting of the upper and lower levels of ^2E state are called $2\bar{A}$ and $\bar{E}$, respectively, and the frequency between them is 29 cm^{-1}.[25,43] By optical pumping the ruby grain from $^4A^2$ state to $2\bar{A}$ state at low temperature using a ruby laser operated at R_2 line (693.9 nm), the laser emission between $2\bar{A}$ and $\bar{E}$ states in terahertz band is expected.[25,43] The rate equations for active medium are as follows:[25]

$$\frac{dN_3(x,t)}{dt} = P_r N_1(x,t) - \frac{N_3(x,t)}{\tau_{31}} - \frac{N_3(x,t)}{\tau_{32}} + \frac{N_2}{\tau_p} + \frac{E}{\hbar\omega_l}\frac{dP_{transition}}{dt}, \tag{7}$$

$$\frac{dN_2(x,t)}{dt} = -\frac{N_2(x,t)}{\tau_{21}} + \frac{N_3(x,t)}{\tau_{32}} - \frac{N_2}{\tau_p} - \frac{E}{\hbar\omega_l}\frac{dP_{transition}}{dt}, \tag{8}$$

$$\frac{dN_1(x,t)}{dt} = -P_r N_1(x,t) + \frac{N_2(x,t)}{\tau_{21}} + \frac{N_3(x,t)}{\tau_{31}}, \tag{9}$$

where N_i (i = 1–3) are the population density in level i; $1/\tau_{ij}$ is the spontaneous decay rate from level i to level j. τ_p is the time of flight between emission and re-absorption of a 29 cm^{-1} phonon. P_r is pumping rate which is proportional to the pump power and is assumed to be constant here. The $\omega_l = (E_3 - E_2)/\hbar$ is lasing frequency between levels 2 and 3; the term $\frac{E}{\hbar\omega_l}\frac{dP_{transition}}{dt}$ is responsible for stimulated emission. For single electron case, the polarization density is related to the population inversion by:[13,14,25]

$$\frac{d^2P_{transition}(x,t)}{dt^2} + \Delta\omega_l \frac{dP_{transition}(x,t)}{dt} + \omega_l^2 P_{transition}(x,t) = k\Delta N(x,t)E(x,t), \tag{10}$$

where $\Delta\omega_l = 1/\tau_{32} + 2/\tau_2$ is full width at half maximum of line-width of atomic transition; τ_2 is the mean time between de-phasing events; $\Delta N = N_2 - N_3$ is the population inversion and $k = 6\pi\varepsilon_0 c^3/\omega_l^2\tau_{32}$ is a constant. The amplification line-shape derived from Eq. (10) is Lorentzian homogeneously broadened when ΔN is independent of time.

The values of those parameters that will be used in our simulation are taken as $\tau_{32} = 1.1 \times 10^{-9}$ s, $\tau_{31} = 3 \times 10^{-6}$ s, $\tau_{21} = 3 \times 10^{-3}$ s, $N = \sum_{i=1}^{3} N_i = 1 \times 10^{24}\ m^{-3}$ and $\nu_l = \omega_l/2\pi = 0.87$ THz ($\lambda_l = 344\ \mu$m).[25] The values of τ_2 and P_r are selected as 2.36×10^{-12} s and $0.32\ s^{-1}$. The high temperature superconductor YBCO is considered in the following calculations. Its parameters in normal state are $\omega_p = 1.67 \times 10^{15}$ rad/s, $\gamma_p = 1.34 \times 10^{13}$ rad/s, and $T_c = 91$ K.[44] When the active system is pumped, the electromagnetic fields can be calculated using FDTD method to solve Eqs. (1), (2), and (7)–(10). In order to simulate an open system, absorbing boundary condition (ABC) is used. Due to numerically solving of Maxwell's equations, boundary conditions for the fields at the interface between two media are automatically satisfied. The space and time increment are taken to be $\Delta x = 1\ \mu$m and $\Delta t = 1.67 \times 10^{-15}$ s, respectively. A Gaussian electromagnetic pulse with an arbitrary amplitude and duration time of 10^{-14} s is used to simulate spontaneous emissions in the system. The electric field is recorded after 8×10^5 Δt, during a time window of length of 2×10^5 Δt at all nodes in the system. By taking the Fourier transform of recorded fields, emission spectrum (electric field intensity) is obtained.[13]

III. RESULTS AND DISCUSSION

In order to determine the effect of temperature on the random lasers consisting of superconductor layers, we consider the one-dimensional RL at different values of α ranging from 0 to 1. First, the value of α is set to be equal to zero which corresponds to pure metallic state ($T = T_c = 91$ K). The spectral intensity is calculated and the corresponding result is shown in Fig. 2(a). One can see that there are three peaks in the emission spectrum with wavelengths of $\lambda_1 = 339.6\ \mu$m, $\lambda_2 = 344.3\ \mu$m, and $\lambda_3 = 359.2\ \mu$m. Despite the wavelength of mode 2 is closer to the gain center wavelength than mode 1, its emission peak is lower. This effect is due to the lower quality factor of the cavities with resonance wavelength of λ_2 than ones with resonance wavelength of λ_1.

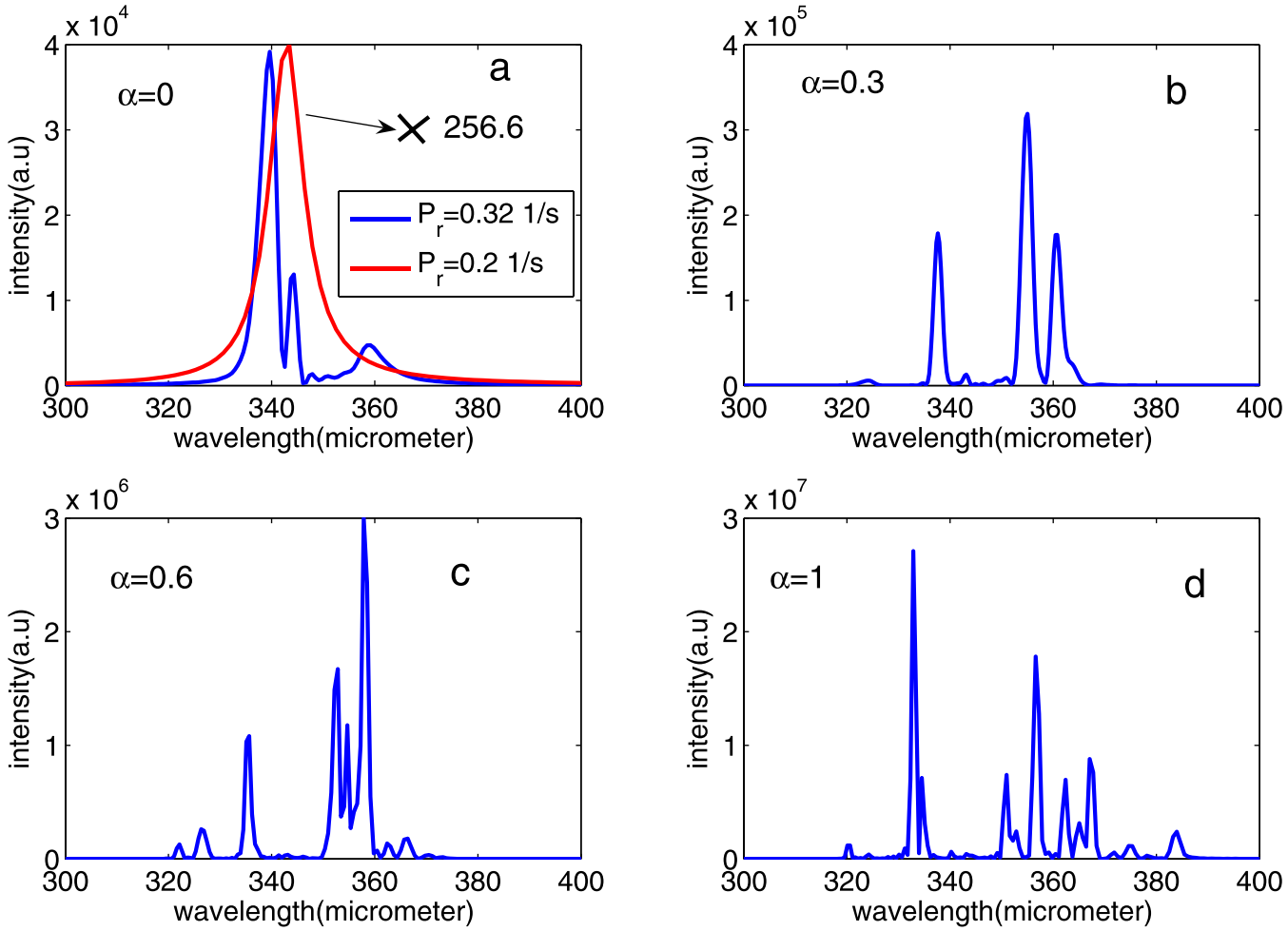

FIG. 2. The spectral intensity in arbitrary units versus wavelength for various values of α: (a) $\alpha = 0$ (for two cases with pumping rate $P_r = 0.2\,s^{-1}$ and $P_r = 0.32\,s^{-1}$); (b) $\alpha = 0.3$ ($P_r = 0.32\,s^{-1}$); (c) $\alpha = 0.6$ ($P_r = 0.32\,s^{-1}$); (d) $\alpha = 1$ ($P_r = 0.32\,s^{-1}$).

For this case, we also calculate the emission spectrum at a lower pumping rate of $0.2\,s^{-1}$ (below the threshold) and the corresponding result is shown in Fig. 2(a) (the curve with red color). One can see that there is a single broad peak in the emission spectrum at this low pumping rate. As the pumping rate increases to $0.32\,s^{-1}$, number of peaks and their intensities increase, while their linewidth reduces. These effects confirm that lasing phenomenon occurs in the system. Note that the pumping rate threshold is determined by checking out the curve of intensity or linewidth of different modes versus pumping rate.[25] The pumping rate is $0.32\,s^{-1}$ for other cases corresponding to other values of α. As shown in Fig. 2(b), with increasing the value of α to 0.3 ($T = 76.14\,K$) five laser peaks are found in the emission spectrum. The wavelengths of the five lasing modes are 324.2, 337.6, 343.1, 355, and 360.5 μm, respectively. Comparison of Fig. 2(a) with Fig. 2(b) reveals that the number of emission peaks and their intensity increase with decreasing the temperature. The strongest peak in Fig. 2(b) is approximately one order of magnitude larger than that in Fig. 2(a). Figs. 2(c) and Fig. 2(d) show the simulated emission spectrum of the designed 1D superconductor based RL (SCRL) with $\alpha = 0.6$ ($T = 57.55\,K$) and $\alpha = 1$ ($T = 0\,K$), respectively, while other parameters are the same as ones in previous cases. Similar trend is observed that as the α value increases, the number of lasing modes and their emitted intensity are increased. It is clear from Fig. 2 that when the α value increases by 0.3, the intensity of the strongest peak increases one order of magnitude. To show the effect of gain on the random system, resonance modes of the passive systems corresponding to the case $\alpha = 0$ are calculated and presented in Fig. 3(a). To calculate the resonance modes, it is sufficient to solve Eqs. (2) and (3) for the systems by setting $P = 0$.[18] In Fig. 3(b), we also plot the curve shown in Fig. 2(a) (blue curve) in a broader wavelength range. As shown in Fig. 3(a), the resonance modes are distributed in a broad range of wavelengths, while lasing modes in Fig. 3(b) are located in the vicinity of gain center wavelength (344 μm). This is because only the modes whose resonance wavelengths are closer to the maximum of the gain spectrum have enough gain to lase. We also perform some calculations on the basis of harmonic inversion method[18,45,46] and find the quality factors of resonance modes with wavelength near 344 μm increase with increasing the α value.

In contrast to conventional lasers, random lasers do not have any traditional cavities and their lasing modes result from eigenstate of disordered media.[47] On the other hand, the quality factors of lasing modes in random lasers are

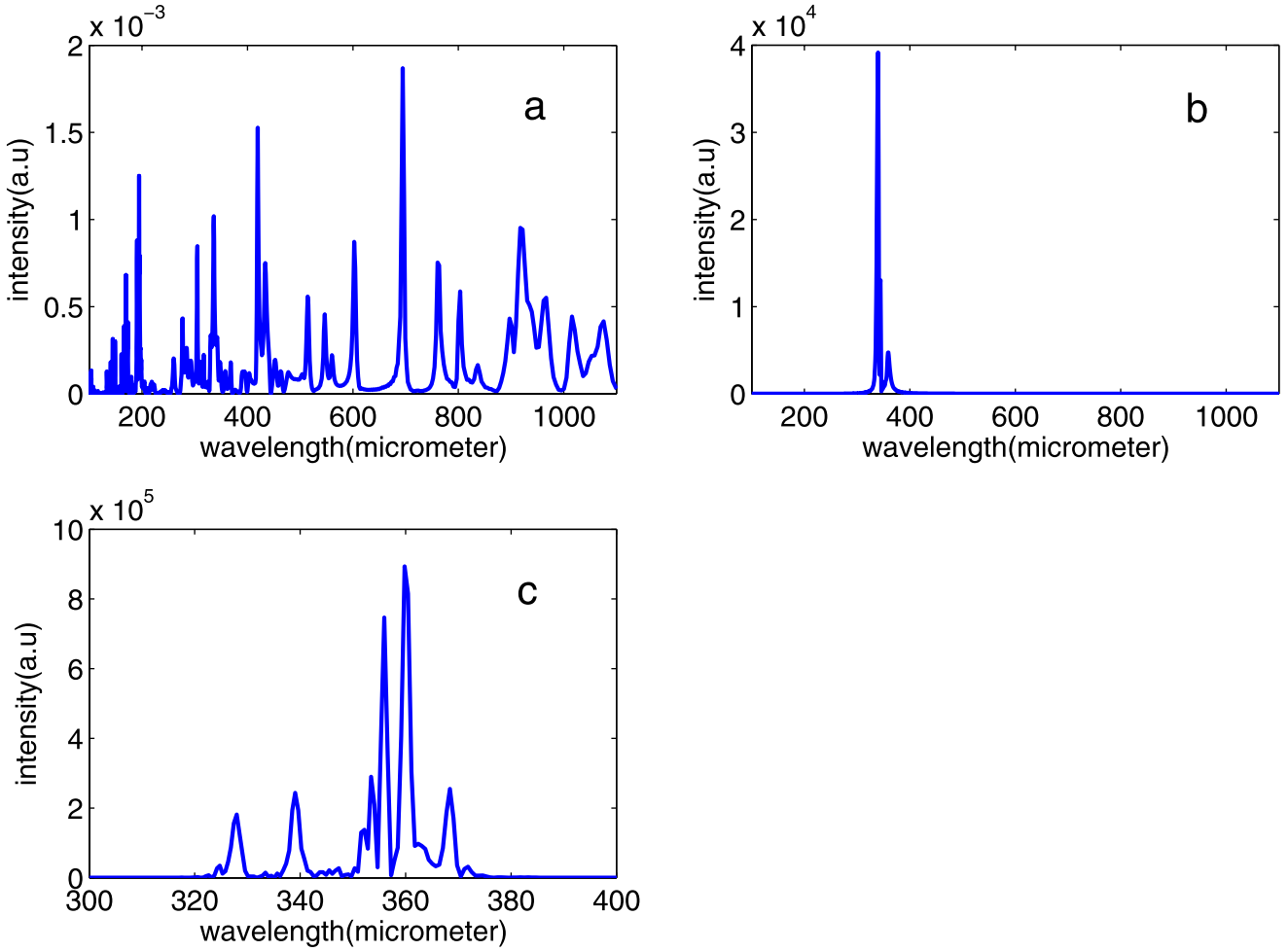

FIG. 3. Spectrum corressponding the fourier transform of the field amplitude of the passive medium (a); the spectral intensity in arbitrary units versus wavelength for the case $\alpha = 0$ in a broader wavelength range at pumping rate of $0.32\,s^{-1}$ (b); the spectral intensity in arbitrary units versus wavelength for the case of $\alpha = 0$ at the pumping rate of $0.4\,s^{-1}$ (c).

lower than those in conventional lasers. Therefore, modes of random lasers are broader than those of regular lasers. When the linewidth of the adjacent modes is larger than the spacing between them, the modes appear as a single broad mode in the emission spectrum. The linewidth of different emission peaks in Fig. 2 is in the range 0.7 μm to 4 μm, which is close to that obtained in Ref. 25. As the value of pumping rate increases, the gain of the modes are improved and new narrow peaks emerge in the previous single mode. To show this effect, for the case $\alpha = 0$, the pumping rate value is increased to $0.4\,s^{-1}$ and corresponding result is shown in Fig. 3(c). One can see that the linewidth of the lasing modes decreases, while their intensity increases. It is also clear from Fig. 2 that emission peaks become narrower with decreasing the temperature. This is because the quality factor of the laser modes increases with decreasing the temperature.

Fig. 4 apparently displays the above mentioned dependence of laser mode wavelength and intensity at the ambient temperature. For the case of $T = 0\,K$, there are 13 laser modes, while the number of laser modes is 3 for the case of $T = 91\,K$. Therefore, the spectral intensities of SCRLs are very sensitive to the system temperature, indicating that the large tunability of the proposed THz random laser with temperature is possible.

Random laser operation is based on Anderson localization and laser amplification cooperation. Anderson localization of electromagnetic wave which provides the feedback in coherent random lasers requires the high refractive index

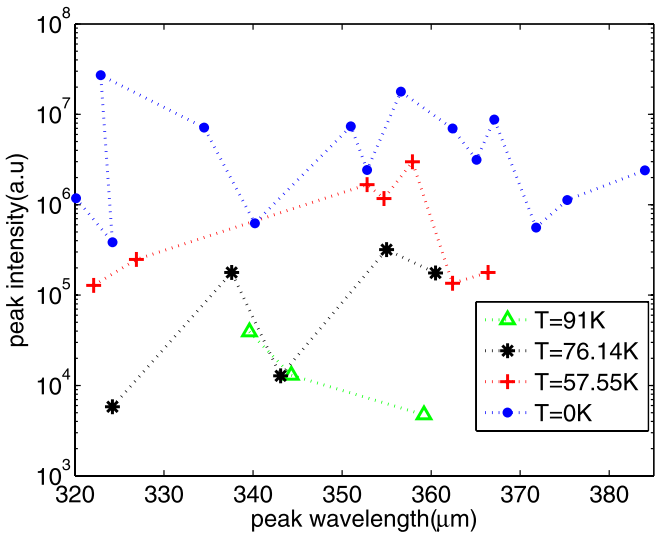

FIG. 4. Intensity and wavelength of different modes in random laser system at different system temperatures.

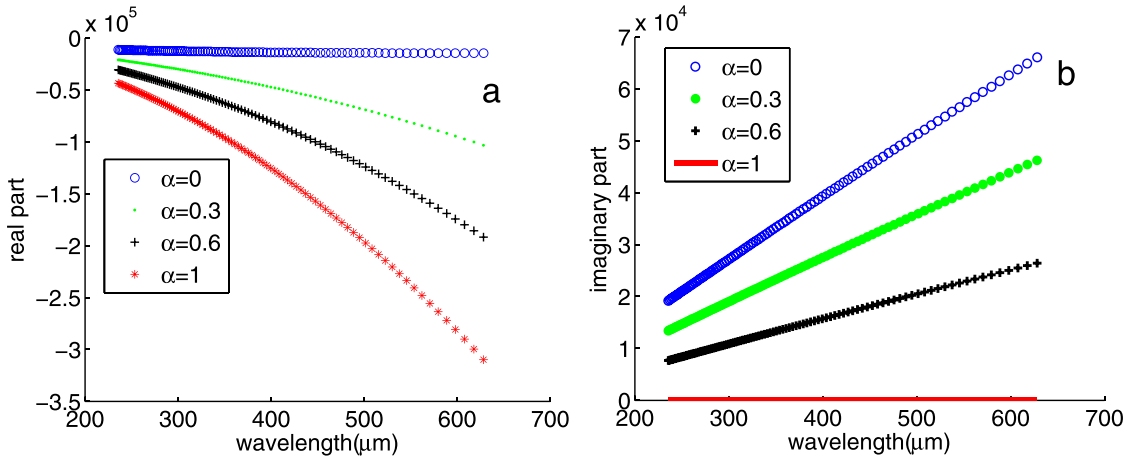

FIG. 5. The real part (a) and imaginary part (b) of the dielectric constant of YBCO layer versus wavelength.

contrast between gain and dielectric media. The loss and scattering coefficients are two factors that determine the quality factor of the resonance cavities in amplifying random media. The contrast between real part of electric permittivity of passive and active media affects on the scattering coefficient and the loss depends on the imaginary part of dielectric constant. To elucidate the mechanism of the observed tunability of SCRLs, we plot the real and imaginary parts of dielectric constant of YBCO as a function of wavelength in the vicinity of gain center wavelength (344 μm) at different temperature in Figs. 5(a) and 5(b), respectively (on the basis of Eq. (5)). One can see that the real part of dielectric constant is negative in this frequency range whose absolute value increases with decreasing temperature. To determine whether or not the above tunability resulted from the variation of the real part of dielectric constant, the effect of absorption is eliminated from Eq. (5) and the numerical calculations are again performed at different temperatures. Our simulation results show that in this case the change in temperature has no significant effect on the emission spectrum. That is, by neglecting the absorption effect in superconductor, temperature controllability of lasing emission disappears. As a result, change in the large negative real part of dielectric constant does not lead to a large variation of quality factor of the formed cavities in the disordered medium. This confirms that the tunability of SCRL through changing the temperature is due to dependence of imaginary part of dielectric constant to the temperature. As shown in Fig. 5(b), when temperature is raised, the imaginary part becomes larger. The imaginary part enhancement causes an increase in the absorption coefficient which reduces the quality factor of the local laser cavities. It is well known that a resonance mode starts lasing when cavity gain balances the total cavity loss. In Fig. 2(a), the absorption coefficient is large, so only those modes which have enough gain or very large quality factor can be excited. Since the modes whose frequencies are closer to center gain frequency have larger gain, and it is expected that laser frequencies appear in the vicinity of gain center frequency and the number of them is small. These effects are clearly observable from Fig. 2(a). As the temperature is decreased, the absorption coefficient becomes smaller so that the quality factor of the cavities is improved. Therefore, even the cavities have low gain and their resonance wavelength is far from the gain center wavelength can meet the threshold condition. This effect leads to the existence of lasing mode with wavelength longer than 360 μm in Figs. 2(c) and 2(d). In addition, due to the enhancement of cavity quality factors with increasing α value, the laser emission becomes more intensive (see Figs. 2(a)–2(d)).

To study the effect of temperature variation on the spatial distribution of electric field in the SCRLs, the electric field in every point of random system is calculated in $t = 1 \times 10^6$ Δt at different temperatures. The calculated results are presented in Fig. 6. As shown in Fig. 6(a), when the YBCO is in the pure metal state ($\alpha = 0$), there are only three localization centers. These localization centers correspond to local cavities in which lasing operation occurs. As shown in Fig. 6, when temperature decreases, more localization centers appear in the system length. Since the system is in the localized regime, each lasing mode is localized around its localization center. As described above, the number of lasing modes increases with α. So, we expect that an increase in the number of localization center occurs with decreasing the temperature. Therefore, the results presented in Fig. 6 are in agreement with those in Fig. 2. On the other hand, variation of the electric field pattern with environment temperature can be applied for remote temperature sensing by direct remotely probing the emission pattern using a telescope without measuring the spectral intensity.[48] To know whether the obtained results is universal or not, we perform many calculations for random systems with different configurations and sizes. Although the number of laser modes, their central frequency, and the exact position of the localization centers depend on the length and configuration of the disordered system, our results confirm that the above obtained results are universal and the observed tunability does not depend on the random system configuration and size.

Consequently, large tunability of SCRLs can be expected due to the transition from the superconducting state to the normal state under the influence of temperature. The experimental realization of this kind of tunable THz SCRL seems sound, which not only provides a THz coherent source

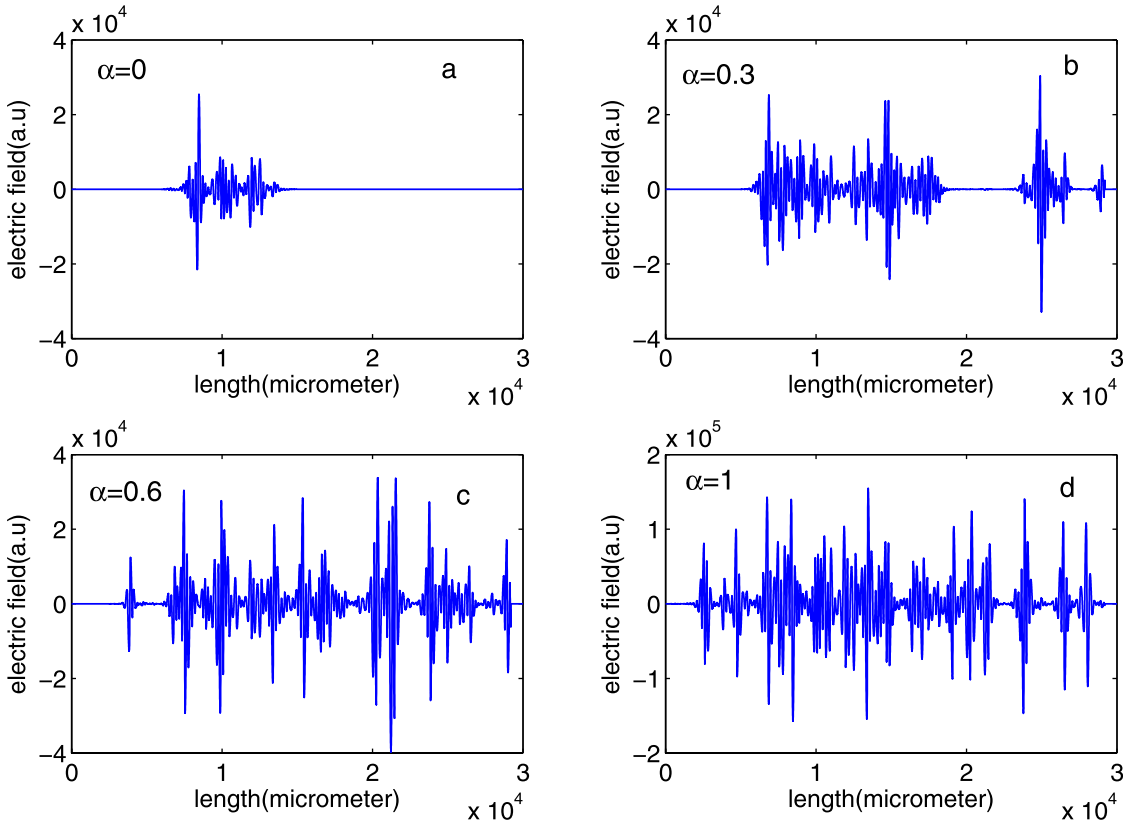

FIG. 6. Spatial distribution of electric field versus the length of system corresponding to various values of α: (a) α = 0, (b) α = 0.3, (c) α = 0.6, (d) α = 1.

but also make possible to study the localization of electromagnetic waves in terahertz domain.

IV. CONCLUSIONS

We have shown that RLs with both superconductor and ruby grain constituents can be made tunable in terahertz domain under the effect of temperature variation. By employing the FDTD method, a one-dimensional random lasing system has been studied at the different temperatures. It is found that transition from metal state to normal state significantly affects on the laser characteristics. The number of lasing modes and their intensity increase with decreasing temperature. It is also observed that more localization centers appear at lower temperatures.

[1]V. S. Letokhov, Sov. Phys. JETP **26**, 835–840 (1968).
[2]V. M. Markushev, V. F. Zolim, and Ch. M. Briskina, Sov. J. Quantum Electron **16**, 281 (1986).
[3]N. M. Lawandy, R. M. Balachandra, A. S. L. Gomes, and E. Sauvain, Nature (London) **368**, 436 (1994).
[4]N. M. Lawandy and R. M. Balachandra, Nature **373**, 204 (1995).
[5]H. Cao, Y. G. Zhao, S. T. Ho *et al.*, Phys. Rev. Lett. **82**, 2278 (1999).
[6]Y. Chen, J. Herrnsdorf, B. Guilhabert, Y. Zhang, I. M. Watson, E. Gu, N. Laurand, and M. D. Dawson, Opt. Express **19**, 2996 (2011).
[7]D. S. Wiersma and A. Lagendijk, Phys. Rev. E **54**, 4256 (1996).
[8]D. Wiersma, Nature **406**, 132 (2000).
[9]X. Y. Jiang and C. M. Soukoulis, Phys. Rev. E **65**, 025601 (2002).
[10]Y. M. Xie and Z. D. Lius, Phys. Lett. A **341**, 339 (2005).
[11]H. E. Tureci, L. Ge *et al.*, Science **320**, 643 (2008).
[12]A. Ghasempour Ardakani, M. Golshani Gharyeh Ali, S. M. Mahdavi, and A. R. Bahrampour, Opt. Laser Technol. **44**, 969 (2012).
[13]X. Jiang and C. M. Soukoulis, Phys. Rev. Lett. **85**, 70 (2000).
[14]P. Sebbah and C. Vanneste, Phys. Rev. B **66**, 144202 (2002).
[15]C. Wang and J. Liu, Phys. Lett. A **353**, 269 (2006).
[16]H. Fujiwara, Y. Hamabata, and K. Sasaki, Opt. Express **17**, 3970 (2009).
[17]J. Lu, J. Liu, H. Liu, K. Wang, and S. Wang, Opt. Commun. **282**, 2104 (2009).
[18]A. Ghasempour Ardakani, A. R. Bahrampour, S. M. Mahdavi, and M. Golshani Gharyeh Ali, Opt. Commun. **285**, 1314 (2012).
[19]A. W. M. Lee, Q. Qin, S. Kumar, B. S. Williams, Q. Hu, and J. L. Reno, Appl. Phys. Lett. **89**, 141125 (2006).
[20]J. R. Gao, J. N. Hovenier, Z. Q. Yang, J. J. A. Baselmans, A. Baryshev, B. S. Williams, S. Kumar, Q. Hu, and J. L. Reno, Appl. Phys. Lett. **86**, 244104 (2005).
[21]H.-W. Hübers, S. G. Pavlov, H. Richter, A. D. Semenov, L. Mahler, A. Tredicucci, H. E. Beere, and D. A. Ritchie, Appl. Phys. Lett. **89**, 061115 (2006).
[22]R. Köhler, A. Tredicucci, H. E. Beere, E. H. Lienfield, A. G. Davis, D. A. Ritchie, R. C. Iotti, and F. Rossi, Nature (London) **417**, 156 (2002).
[23]A. Benz, Ch. Deutsch, G. Fasching, K. Unterrainer, A. M. Andrews, P. Klang, W. Schrenk, and G. Strasser, Opt. Express **17**, 941 (2009).
[24]X. Li-Hong, M. L. Ronald, E. C. C. Vasconcellos, S. C. Zerbetto, L. R. Zink, and K. M. Evenson, IEEE J. Quantum Electron. **32**, 392 (1996).
[25]J. Liu, Y. Liu, J. Lu, and K. Wang, Opt. Express **18**, 22880 (2010).
[26]N. M. Lawandy, Brown University Research Foundation, WO 00038283, 2000.
[27]D. S. Wiersma and S. Cavalieri, Nature (London) **414**, 708 (2001).
[28]S. Gottardo, R. Sapienza, P. D. Garcia, A. Blanco, D. S. Wiersma, and C. Lopez, Nat. Photonics **2**, 429 (2008).
[29]C. R. Lee, J. D. Lin, B. Y. Huang, S. H. Lin, T. S. Mo, S. Y. Huang, C. T. Kuo, and H. C. Yeh, Opt. Express **19**, 2391 (2011).
[30]A. Ghasempour Ardakani, M. Hosseini, A. R. Bahrampour, and S. M. Mahdavi, Opt. Commun. **285**, 1900 (2012).
[31]H. Ming Lee and J. C. Wu, J. Appl. Phys. **107**, 09E149 (2010).
[32]Yu. E. Lozovik, S. L. Eiderman, and M. Willander, Laser Phys. **17**, 1183 (2007).
[33]A. H. Aly, S. W. Ryu, H. T. Hsu, and C. J. Wu, Mater. Chem. Phys. **113**, 382 (2009).
[34]H. Takeda and K. Yoshino, Phys. Rev. B **67**, 245109 (2003).
[35]H. Takeda, K. Yoshino, and A. A. Zakhidov, Phys. Rev. B **70**, 085109 (2004).
[36]H. T. Hsu, F. Y. Kuo, and C. J. Wu, J. Appl. Phys. **107**, 053912 (2010).

[37]C. J. Gorter and H. G. B. Casimir, Phys. Z. **35**, 963 (1934).
[38]Yu. E. Lozovik and S. L. Éoederman, Metals and Superconductors **50**, 2024 (2008).
[39]J. Bardeen, Phys. Rev. Lett. **1**, 399 (1958).
[40]J. Rammer, Europhys. Lett. **5**, 77 (1988).
[41]J. M. Pond, K. R. Carroll, J. S. Horowitz, D. B. Chrisey, M. S. Osofsky, and V. C. Cestone, Appl. Phys. Lett. **59**, 3033 (1991).
[42]O. G. Vendik, I. B. Vendik, and D. I. Kaparkov, IEEE Trans. Microwave Theory Tech. **46**, 469 (1998).
[43]E. Kuznetsova, Y. Rostovtsev, N. G. Kalugin, R. Kolesov, O. Kocharovskaya, and M. O. Scully, Phys. Rev. A **74**, 023819 (2006).
[44]A. N. Poddubnya, E. L. Ivchenkoa, and Yu. E. Lozovikb, Solid State Commun. **146**, 143 (2008).
[45]V. A. Mandelshtam and H. S. Taylor, J. Chem. Phys. **107**, 6756 (1997).
[46]V. A. Mandelshtam and H. S. Taylor, J. Chem. Phys. **108**, 9970 (1998).
[47]H. Cao, X. Jiang, Y. Ling, J. Y. Xu, and C. M. Soukoulis, Phys. Rev. B **67**, 161101 (2003).
[48]D. S. Wiersma, Nature **4**, 359 (2008).